Connectivity of Highway Vehicular Networks

Marco Gramaglia, Oscar Trullols-Cruces, Diala Naboulsi, Marco Fiore, Maria Calderon

Connectivity of Highway Vehicular Networks

Marco Gramaglia[1] and Oscar Trullols-Cruces[2] and Diala Naboulsi[3] and Marco Fiore[4,3] † and Maria Calderon[5]

[1]*Istituto Superiore Mario Boella, Torino, Italy*
[2]*Universitat Politècnica de Catalunya, Barcelona, Spain*
[3]*INRIA, Université de Lyon, INSA-Lyon, CITI-INRIA, F-69621, Villeurbanne, France*
[4]*CNR-IEIIT, Torino, Italy*
[5]*Universidad Carlos III, Madrid, Spain*

Il y a un besoin croissant de jeux de données de mobilité pour l'évaluation de architectures et protocoles réseaux conçus pour les environnements véhiculaires. Tels jeux données doivent être réalistes, accessibles à la communauté scientifique, ainsi que hétérogènes – c'est à dire, ils doivent capturer le trafic routier dans des conditions variés. Nous contribuons à l'effort pour définir des nouveaux scénarios de mobilité qui respectent ces pré-requis, en introduisant un ensemble de traces de mobilité pour la simulation des réseaux véhiculaires, dérivées de mesures à haute résolution des flux de traffique réels sur deux autoroutes autour de la ville de Madrid, en Espagne. Nous évaluons leur intérêt en caractérisant la connectivité des réseaux véhiculaires construits sur les différentes traces. Nos résultats soulignent l'impact important des variations de la portée radio entre les véhicules. En outre, ils dévoilent les dynamiques temporelles de la topologie des réseaux véhiculaires en environnement autoroutier, et en identifient les causes.

Keywords: vehicle-to-vehicle communications, vehicular networks, mobility modeling, connectivity analysis.

1 Introduction

Despite the fact that technologies based on Dedicated Short-Range Communication (DSRC) and the associated services will soon hit the market, the vast majority of applications, protocols and architectures for upcoming vehicular networks is still evaluated via simulative studies. Within such a context, the level of realism of the simulation is a paramount aspect to account for, and the way the mobility of individual vehicles is represented is often the single feature that introduces the largest bias in the results.

During the past decade, there have been efforts aiming at gathering real-world road traffic data,developing tools for the simulation of vehicular movement.and generating synthetic mobility datasets.This notwithstanding, there is still a noticeable scarcity of road traffic datasets featuring the level of realism and of spatiotemporal granularity required for network simulation.The result of the lack of a set of realistic, publicly shared, heterogeneous scenarios is that simulations of vehicular networks are often unreliable and non-reproducible.

We contribute to the endeavor of enlarging the set of realistic datasets of vehicular mobility that are freely available to the research community. To that end, we present 16 original traces describing the road traffic on two highways around Madrid, Spain, at different times of multiple weekdays. The traces are derived from high-detail real-world traffic counts, and describe unidirectional free-flow traffic in quasi-stationary conditions on a road spanning over 10 km. We then provide a characterization of the vehicular network connectivity in the synthetic traces, investigating the impact of time (i.e., hour of the day, day of the week), highway diversity, and vehicular communication range. Our results highlight that : (i) the level of global vehicular connectivity can be primarily ascribed to the V2V communication range ; (ii) for short communication ranges, the vehicular connectivity is driven by a mixture of slow and fast temporal dynamics that are regulated by the road traffic density and by V2V contact durations, respectively.

†The research leading to these results has received funding from the People Programme (Marie Curie Actions) of the European Union's Seventh Framework Programme (FP7/2007-2013) under REA grant agreement n.630211.

(a) Locations (b) M40 - Measurement point (c) A6 - Measurement point (d) M40 - Induction loop

FIGURE 1: Geographical location of the two highways near Madrid, Spain (a). Close-by view of measurement points (b,c), and of the induction loop on M40 (d).

2 Data collection

The empirical data used throughout this work comes from measurement locations in the region of Madrid, Spain. The data, kindly provided to us by the Spanish office for the traffic management (Dirección General de Tráfico, DGT), detail road traffic conditions on two arterial highways.

The *M40* is part of the middle layer of the Madrid city beltway system, which also comprises M-30 (innermost) and M-50 (outermost). This beltway, which has an average distance of 10.7 km from the city center, traverses both the most peripheral areas of the municipality and surrounding cities. The measurement point is placed at the 12.7-km milepost, where the M40 traverses the suburb of San Blas and the town of Coslada. The measures cover the internal carriageway (southbound) that includes 3 lanes with a speed limit of 100 km/h. The M40 is indicated as A in Fig. 1(a), while a photographic view of the exact measurement location is provided in Fig. 1(b).

The Autovía *A6* is a motorway that connects the city of A Coruña to the city of Madrid. This road enters into the urban area from the northwest and collects the traffic demand of the conurbation that was built along it. The data collection point is placed around the 11-km milepost (Madrid direction), where the A6 features three lanes with a speed limit of 120 km/h. We remark, however, that this location is right after a popular entrance ramp that joins the rightmost lane and significantly slows down the road traffic. The highway maps to B in Fig. 1(a). A photographic view of the collection point is in Fig. 1(c).

The sensors that DGT deployed on M40 and A6 are induction loops. They consist of loops of wires buried under the concrete layer that create a magnetic field. When a vehicle passes on the vertical axis of the loop, it creates a variation in the magnetic field, which is considered as a new transit. If two loops are placed close to each other, also the vehicular speed (and possibly other metrics, such as the vehicle length) is obtained. A picture of the buried induction loops used to collect measurements on the M40 is shown in Fig. 1(d).

Usually, these devices are programmed to supply coarse-grained data, as public transportation authorities are generally interested in aggregate measures, (e.g., the number of vehicles transiting on a road, their average speed, or the percentage of heavy vehicles) so as to detect exceptional alterations in the road capacity.The loops installed by DGT were configured to supply data averaged over 60-second intervals, but their configuration was changed specifically for our study : the real-world traffic counts we collected provide fine-grained time, speed and lane information on each single transiting vehicle. To the best of our knowledge, this is the most precise traffic count dataset recorded to date, and represents an ideal input to our microscopic simulation of highway traffic.

The timing of the data collection is a very important variable to account for, since vehicular traffic presents, as many other human activities, important temporal variability : for instance, rush hours yield diverse traffic conditions than off-peak hours, especially on main arterial roads like those we consider. The dataset analyzed in this work was collected on multiple days of May 2010, namely Friday the 7th, Monday the 10th, Tuesday the 11th, and Wednesday the 12th. For each measurement location and each day, two traces are available : one capturing the traffic peak (from 8 :30 a.m. to 9 :00 a.m.), and one during off-peak hours (from 11 :30 a.m. to 12 :00 p.m.). As a result, our empirical dataset provides a heterogeneous view of traffic conditions, allowing us to generate synthetic mobility traces that are representative of different highway congestion levels.

Model	Parameter	Meaning	Value
IDM	a	Maximum acceleration	1 m/s^2
IDM	b	Maximum (absolute) deceleration	2.5 m/s^2
IDM	v_i^{max}	Maximum desired speed	$\sim f_V(v)$
IDM	Δx_{safe}	Minimum safety distance	1 m
IDM	Δt_{safe}	Minimum safe time headway	0.65 s
MOBIL	p	Politeness factor	0.5
MOBIL	a_L	Bias acceleration (left)	0 m/s^2
MOBIL	a_R	Bias acceleration (right)	0.2 m/s^2
MOBIL	k	Hysteresis threshold factor	0.3

TABLE 1: IDM and MOBIL parameter settings.

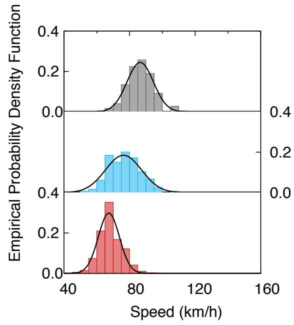

FIGURE 2: Per-lane $f_V(v)$ on A6, 8 :30 a.m.

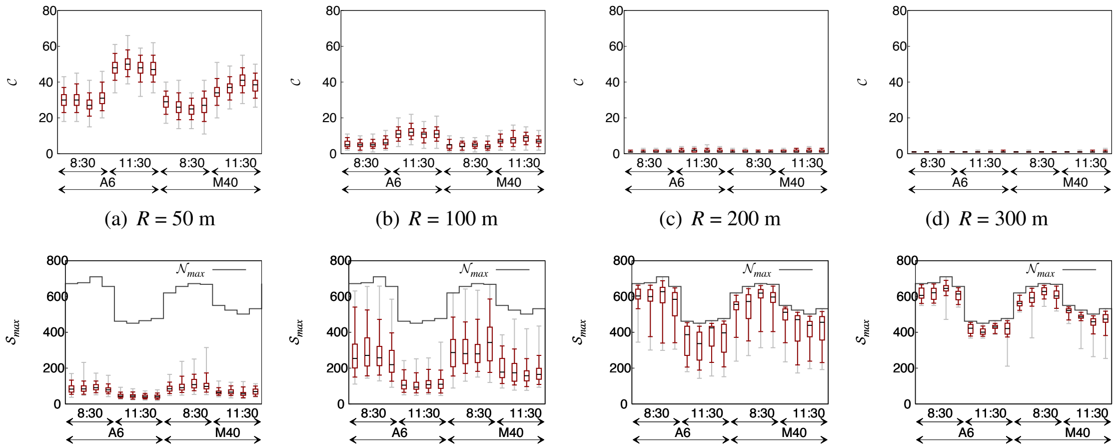

(a) $R = 50$ m (b) $R = 100$ m (c) $R = 200$ m (d) $R = 300$ m

(e) $R = 50$ m (f) $R = 100$ m (g) $R = 200$ m (h) $R = 300$ m

FIGURE 3: Candlestick istributions of $\mathcal{C}$ (top), and $\mathcal{S}_{max}$ (bottom), for each mobility trace under different values of R.

3 Dataset generation

Our objective is to generate road traffic traces that are representative of unidirectional free flow highway traffic in a quasi-stationary state, i.e., such that comparable traffic conditions are present in between the in-flow and out-flow boundaries of the simulated highways. The datasets should cover a geographical distance that is sufficient for networking studies (e.g., for warning message dissemination or floating car data upload). In the following, we simulate a 10-km road segment, but we remark that our approach can easily accommodate shorter or longer highway stretches.

In order to achieve the goal above, we fed the real-world traffic count data presented in Sec. 2 to a microscopic vehicular mobility simulator based on well-known models of car-following and lane-changing behaviors of individual drivers. Specifically, we employed the Intelligent Driver Model (IDM) [1] to characterize the instantaneous acceleration of each vehicle, and the Minimizing Overall Braking Induced by Lane-changes model (MOBIL) [2] to represent inter-lane movement decisions.

In order to obtain quasi-stationary traffic conditions over the simulated highway segment, some calibration of the IDM and MOBIL parameters proved necessary. Specifically, for the acceleration a, deceleration b, politeness factor p and minimum safety distance Δx_{safe} we could use the default values suggested in [1,2]. The other parameters had instead to be adapted to the specificities of each road scenario. The final IDM and MOBIL settings are summarized in Tab. 3, where $f_V(v)$ is a Gaussian-shaped distribution of maximum desired speed, which is calibrated from empirical per-lane free-flow ingress velocities. Therefore, the exact parameters of $f_V(v)$ depend on the considered scenario. As an example, distributions for the three lanes of A6 at 8 :30 a.m. are shown in Fig. 3 : there, the histograms portray empirical per-lane free-flow ingress speed distributions, while the curves map to the fitted $f_V(v)$ normal distributions.

4 Connectivity analysis

We present some results of the connectivity analysis we carried out on the resulting synthetic mobility traces. Specifically, in the following we present results for different values of the vehicle-to-vehicle communication range R, from 50 to 300 meters. These values represent the lower and upper bounds for acceptable packet delivery ratios, according to experimental studies [3,4]. We focus on the distributions of the number of components $\mathcal{C}$ and of the size of the largest component $\mathcal{S}_{max}$. Indeed, $\mathcal{C}$ is a measure of how fractioned the network is, while $\mathcal{S}_{max}$ is the maximum number of nodes that can be reached via multi-hop communication. Clearly, the lower is $\mathcal{C}$ and the larger is $\mathcal{S}_{max}$, the better connected is the vehicular network.

In Fig. 3, we present the distributions of $\mathcal{C}$ (top plots) and $\mathcal{S}_{max}$ (bottom plots), for various values of the communication range R (on different columns). In every plot, each candlestick refers to one mobility trace, and is obtained by aggregating the metrics computed in all instantaneous graphs observed at every second during the 30-minute timespan of that trace. The lowest and highest values in the candlesticks (in grey) are the minimum and maximum values that the metric attains. The inner error bars (in red) depict the first and ninth deciles, while the box highlights the first and third quartiles (in red) around the median value (in black). Also, the step function in the $\mathcal{S}_{max}$ plots is the maximum number of vehicles $\mathcal{N}_{max}$ observed in all instances of the respective trace. It thus represents the upper bound to $\mathcal{S}_{max}$: the closer is $\mathcal{S}_{max}$ to $\mathcal{N}_{max}$, the closer the vehicular network is to a fully connected single component.

Let us now focus on the case of $R = 50$ m, in Fig. 3(a) and Fig. 3(e). We observe that the connectivity metrics are very similar on different days of the week, forming four clear clusters in both plots. This implies that we can expect the network to have consistent topological properties from Monday to Friday. The aforementioned clusters are instead separated by highway (A6 or M40) and hour (8 :30 or 11 :30). Specifically, the network appears more fragmented on A6 than on M40, and, in both cases, the connectivity is worse at 11 :30 a.m. than at 8 :30 a.m. Intuitively, we can ascribe such a variability to the different road traffic conditions encountered on the two highways at different times of the day.

The observations above still hold when considering different communication ranges separately. Nonetheless, when comparing the plots for varying R, it is evident that increasing the communication range can dramatically improve the connectivity of the network. Indeed, for $R = 50$ m, there exist on average 30-50 disconnected components, the largest of which only comprises around one tenth of the vehicles. As R grows, however, the network fragmentation is reduced, and more nodes join the largest component. When $R = 300$ m almost all vehicles belong all the time to one single component, as in Fig. 3(d) and Fig. 3(h). We conclude that *the communication range is the foremost parameter controlling the vehicular network connectivity*, as it can induce variations in $\mathcal{C}$ and $\mathcal{S}_{max}$ that are much more significant than those imputable to road traffic conditions. Indeed, $R = 300$ m guarantees a well connected network independently of the traffic scenario, but reducing that value causes the topology to rapidly break apart.

We also carried out additional topological analyses in presence of communication ranges below 200 m, which are not reported here due to space limitations. Such analyses revealed that the network connectivity undergoes temporal variations that are a combination of slow dynamics, controlled by the road traffic density, and fast dynamics, due to the predominant presence of short-lived contacts. Interestingly, we found such properties to be invariant throughout multiple weekdays and on different highways.

Références

[1] M. Treiber, A. Hennecke, and D. Helbing, "Congested traffic states in empirical observations and microscopic simulations," *Phys. Rev. E*, 62(2) :1805–1824, 2000.

[2] M. Treiber and D. Helbing, "Realistische mikrosimulation von strassenverkehr mit einem einfachen modell," *ASIM*, 2002.

[3] F. Martelli, M. E. Renda, G. Resta, and P. Santi, "A measurement-based study of beaconing performance in IEEE 802.11p vehicular networks," *IEEE INFOCOM*, 2012.

[4] F. Bai, D. D. Stancil, and H. Krishnan, "Toward understanding characteristics of dedicated short range communications (DSRC) from a perspective of vehicular network engineers," *ACM MobiCom*, 2010.